

# A top-down approach to prepare silicoaluminophosphate molecular sieve nanocrystals with improved catalytic activity†

 Cite this: *Chem. Commun.*, 2014, 50, 1845

 Received 29th October 2013,  
 Accepted 16th December 2013

DOI: 10.1039/c3cc48264b

www.rsc.org/chemcomm

 Miao Yang,<sup>a</sup> Peng Tian,<sup>a</sup> Chan Wang,<sup>ab</sup> Yangyang Yuan,<sup>ab</sup> Yue Yang,<sup>a</sup> Shutao Xu,<sup>a</sup> Yanli He<sup>a</sup> and Zhongmin Liu\*<sup>a</sup>

**Silicoaluminophosphate SAPO-34 molecular sieve nanocrystals have been prepared by a post-synthesis milling and recrystallization method, which is further proven to be universally applicable to other SAPO molecular sieves. The obtained SAPO-34 with reduced Si enrichment on the external surface shows considerably improved catalytic performance in the MTO reaction.**

Molecular sieves have been widely used in industries as heterogeneous catalysts.<sup>1</sup> Their regular channel structures, which are in the size range of many molecules, make them excellent shape-selective catalysts.<sup>2</sup> However, the molecular dimension of the micropores may suffer diffusion limitation and cause fast coke deposition.<sup>3</sup> Preparation of nanoscale molecular sieves or hierarchical molecular sieves is considered to be an effective solution, which could improve the catalytic efficiency because of the shortened diffusion paths and increased external surface area.<sup>4</sup>

SAPO-34, one of the most important members in the SAPO family, has exhibited excellent catalytic performance in the methanol-to-olefins (MTO) reaction due to the contribution of the CHA structure, medium/strong acidity, and high hydrothermal stability.<sup>5</sup> It is acknowledged that decreasing the crystal size of SAPO-34 could improve its MTO catalytic lifetime.<sup>6</sup> Therefore, the synthesis of nano-SAPO-34 is very attractive from both academic and practical perspectives. Many synthetic strategies, such as the colloidal solution method,<sup>7</sup> dry gel conversion,<sup>8</sup> microwave,<sup>9</sup> sonochemical<sup>10</sup> and two-step hydrothermal crystallized methods,<sup>11</sup> have been tried to obtain small SAPO-34 crystals. All these processes are bottom-up methods, and involve the use of expensive tetraethylammonium hydroxide (TEAOH) as the template. Other organic templates such as triethylamine (TEA), diethylamine (DEA), and morpholine (MOR) generally lead to micrometer-sized SAPO-34 crystals.

<sup>a</sup> National Engineering Laboratory for Methanol to Olefins, Dalian National Laboratory for Clean Energy, Dalian Institute of Chemical Physics, Chinese Academy of Sciences, Dalian 116023, P. R. China. E-mail: liuzm@dicp.ac.cn

<sup>b</sup> University of Chinese Academy of Sciences, Beijing, P. R. China

† Electronic supplementary information (ESI) available: More details of experimental and characterization processes, TG, XRD, SEM, NH<sub>3</sub>-TPD, <sup>27</sup>Al and <sup>31</sup>P MAS NMR spectra and the MTO reaction catalytic results. See DOI: 10.1039/c3cc48264b

The traditional top-down method has been widely used to create mesopores in aluminosilicate zeolites through post treatment of zeolites in an acidic (dealumination) or basic (desilication) solution.<sup>12</sup> However, it is difficult to employ this method to modify SAPO molecular sieves because the frameworks of SAPOs are not as stable as those of aluminosilicates during acidic/basic treatment. Recently, a novel top-down approach has been proposed to prepare nanosized zeolite A and ZSM-5.<sup>13</sup> The zeolite crystals were first crushed by bead milling. After that, the crystallinity was recovered by recrystallization of the milled precursor in a dilute aluminosilicate solution.

In this work, we successfully developed the post-synthesis milling and recrystallization method to prepare small SAPO-34 crystals. Both the mother liquid collected from SAPO-34 synthesis and the self-made solution could be employed as the recrystallization solution. The obtained SAPO-34 crystallites showed prolonged catalytic lifetime and higher selectivity to light olefins in the MTO reaction.

Micrometer-sized SAPO-34 was first synthesized using DEA as a template according to our previous work.<sup>14</sup> The SAPO-34 precursor was calcined followed by milling using a planetary ball mill with water as a dispersing phase. After that, the milled SAPO-34 was hydrothermally recrystallized in a mother liquid or a self-made aluminophosphate solution at 180 °C for 2–24 hours (Table 1). It should be noted that the small crystal size remained almost unchanged even after recrystallization at 200 °C for 24 hours (Fig. S1, ESI†). The Si

Table 1 Preparation of SAPO-34 by the recrystallization method<sup>a</sup>

Sample	Recrystallization solution P/Al/Si/TEA/H <sub>2</sub> O	Product composition	T (°C)/t (h)
1 <sup>b</sup>	1.5/1/0.08/-/73	Al <sub>0.498</sub> Si <sub>0.116</sub> P <sub>0.386</sub> O <sub>2</sub>	180/2
2 <sup>b</sup>	1.5/1/0.08/-/73	Al <sub>0.485</sub> Si <sub>0.136</sub> P <sub>0.379</sub> O <sub>2</sub>	180/2
3 <sup>b</sup>	1.5/1/0.08/-/73	Al <sub>0.482</sub> Si <sub>0.148</sub> P <sub>0.370</sub> O <sub>2</sub>	180/2
4	1.0/1.0/0/1.9/75	Al <sub>0.575</sub> Si <sub>0.117</sub> P <sub>0.307</sub> O <sub>2</sub>	180/3
5	1.0/1.0/0/1.9/75	Al <sub>0.537</sub> Si <sub>0.124</sub> P <sub>0.339</sub> O <sub>2</sub>	180/24
6	1.0/1.0/0/1.75/27.5	Al <sub>0.508</sub> Si <sub>0.088</sub> P <sub>0.404</sub> O <sub>2</sub>	200/24

<sup>a</sup> SAPO-34 as the precursor (Al<sub>0.448</sub>Si<sub>0.200</sub>P<sub>0.351</sub>O<sub>2</sub>), solid/recrystallization solution mass ratio was 1/15 for sample 1, 1/10 for samples 2, 4–6 and 1/5 for sample 3. <sup>b</sup> Mother liquid as the recrystallization solution, which was obtained from SAPO-34 synthesis using TEA as a template. For more details see ESI.

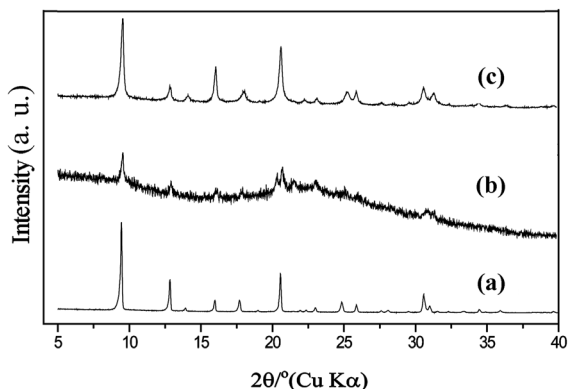


Fig. 1 XRD patterns of (a) SAPO-34 precursor, (b) milled SAPO-34, and (c) recrystallized SAPO-34 (sample 2).

content in the product, which had great effects on the acidity of the sample (catalytic properties), could be tuned by simply modifying the reaction conditions. A similar self-made solution using DEA or MOR as the template could also accomplish the recrystallization, but gave SAPO-34 products with larger crystal size (0.2–2.0 μm). In addition, using NaOH or NH<sub>3</sub>·H<sub>2</sub>O as the basic resource only resulted in the formation of amorphous material or ammonium aluminum phosphate, suggesting that the organic template was necessary for the structure recovery. In fact, TG analysis (Fig. S2, ESI<sup>†</sup>) of sample 2 gave a total weight loss of 17.0 wt% including around 4 wt% water and 13 wt% organic template. This is comparable to that of the conventional SAPO-34, confirming the incorporation of an organic template into the recrystallized product.

The XRD patterns of the SAPO-34 precursor, together with its milled and recrystallized samples, are given in Fig. 1. The precursor showed typical diffraction peaks of CHA structure. The peak intensity of the milled sample decreased a lot indicating a destruction of the crystal structure. Upon recrystallization, the product regained the high quality XRD pattern in spite of some broadening of the peaks, suggesting the recovery of the crystal structure and the reduced particle size. Fig. 2 shows the SEM images of the three SAPO samples. A typical rhombohedral morphology was observed for the SAPO-34 precursor, and the particle size was around 4–8 μm with tiny smaller crystals. After milling, the regular morphology disappeared forming disordered agglomerates instead. Nanoscale particles with cubic-like morphology (50–350 nm in size) could be recognized after recrystallization, in agreement with the XRD results.

The N<sub>2</sub> adsorption properties of the samples are presented in Fig. S3 and Table S2 (ESI<sup>†</sup>). The precursor exhibits typical adsorption properties of SAPO-34, while the milled sample has a very low N<sub>2</sub> adsorption ability suggesting that the CHA structure has been seriously damaged by milling. Notably, the isotherms of recrystallized samples 2 and 6 regain the type-I curve illustrating the rebuilding of microporous structure. The increased external surface area confirmed the small size of the recrystallized product, and the high mesopore volume was associated with multilayer adsorption between the intercrystal pores of nanoparticles, as reflected in the isotherm with an abrupt inclination at relatively high pressure ( $P/P_0 > 0.9$ ).

Solid-state <sup>29</sup>Si, <sup>27</sup>Al, and <sup>31</sup>P MAS NMR spectra were obtained to investigate the local atomic environments in the samples. As shown

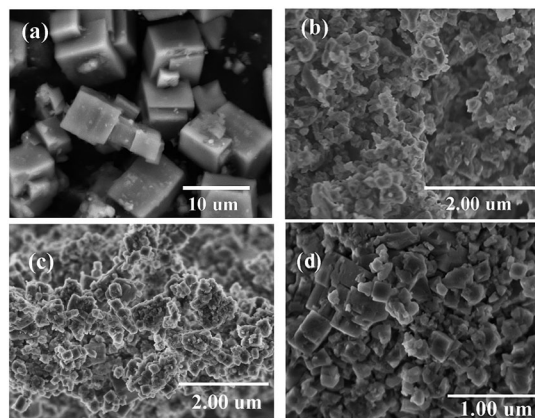


Fig. 2 SEM micrographs of (a) SAPO-34 precursor, (b) milled SAPO-34, and (c and d) recrystallized SAPO-34 (sample 2).

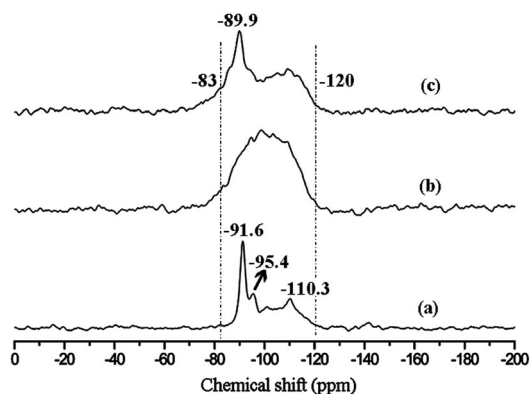


Fig. 3 <sup>29</sup>Si MAS NMR spectra of (a) SAPO-34 precursor, (b) milled SAPO-34, and (c) recrystallized SAPO-34 (sample 2).

in Fig. 3, the <sup>29</sup>Si spectra of the precursor gave one strong peak at -91.6 ppm due to Si(OAl)<sub>4</sub> species, and several overlapped peaks between -95.4 and -110.3 ppm ascribed to Si(OAl)<sub>n</sub>(OSi)<sub>4-n</sub> ( $n = 3-0$ ) species. Only a broad signal was observed in the spectrum of the milled sample, corresponding to its low crystallinity. The <sup>29</sup>Si spectrum of the recrystallized SAPO-34 (sample 2) looked more like a superimposed one from those of the raw and milled samples. The shoulder peaks at -83 and -86 ppm in the spectrum should arise from Si(OAl)<sub>3</sub>(OH) and Si(OAl)<sub>2</sub>(OH)<sub>2</sub> species respectively.<sup>15</sup> Moreover, the broad peaks between -90 and -120 ppm may also contain the contribution of Si species connecting with OH groups. The <sup>27</sup>Al and <sup>31</sup>P spectra of the samples are given in Fig. S4 (ESI<sup>†</sup>). They showed a similar change to the <sup>29</sup>Si spectra after milling and recrystallization treatment where penta- (10 ppm) and hexacoordinated (-10 ppm) Al species and not fully condensed P species (-12 to -20 ppm) can be observed. These results implied that there existed more defects in the recrystallized framework. After calcination, sample 2 exhibited a narrow tetrahedral <sup>27</sup>Al peak like the precursor, indicating that the sample was free of extra-framework Al atoms.

A remarkable feature of the present SAPO-34 crystallites is their improved catalytic properties in the MTO reaction (Fig. 4 and Table S1, ESI<sup>†</sup>). Compared with the performance of the SAPO-34 precursor, the catalytic lifetime of sample 2 was dramatically

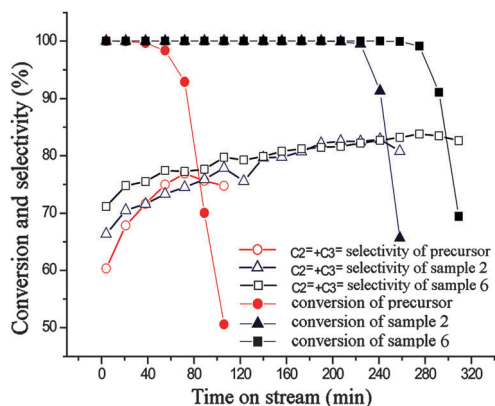


Fig. 4 Methanol conversion and selectivity of C<sub>2</sub>H<sub>4</sub> plus C<sub>3</sub>H<sub>6</sub> in the MTO reaction on the SAPO-34 precursor, sample 2 and 6. Reaction conditions: 450 °C, WHSV = 4.0 h<sup>-1</sup>, 40 wt% methanol solution.

extended from 38 to 224 min, and the selectivity of ethylene plus propylene was increased from 71.6 to 82.6%. Meanwhile, the selectivity to propane (the secondary product from propylene) was reduced from 6.3% to 0.6%. Similar catalytic results were observed for sample 6 recovered from the self-made recrystallization solution, which showed a lifetime of 258 min and 83.2% selectivity of ethylene plus propylene. The catalytic performance of the milled sample was also tested, which showed very low activity (methanol conversion < 5 wt%, Fig. S5, ESI†). NH<sub>3</sub>-TPD experiments were carried out to probe the acid properties of the samples, and the curves are given in Fig. S6 (ESI†). The high-temperature desorption peak for the recrystallized SAPO-34 shifted to lower temperature together with decreased intensity as compared with that of the precursor, suggesting the reduced acid strength and amount. This was consistent with the reduced Si content in the recrystallized samples. Moreover, the surface compositions of the samples were also examined by XPS (Table 2), because of the fact that the Si content and its coordination environment at the crystal surface are very important for the MTO reaction performance.<sup>16</sup> Clearly, there existed an obvious Si enrichment on the external surface of the precursor, reflecting a gradual increase of the Si content in SAPO crystals from the core to the surface.<sup>17</sup> After milling, the Si enrichment phenomenon was weakened due to the exposure of the internal surface to a relatively low Si content. The Si content on the crystal surface was further decreased after recrystallization, and the *R* value (the ratio of Si/(Al + P)<sub>surface</sub> over Si/(Al + P)<sub>bulk</sub>) of the recrystallized samples was obviously lower than that of the precursor, suggesting a weakened surface Si enrichment. This was

Table 2 Elemental composition from XPS analysis

Sample	Surface elemental composition (mol%)			<i>R</i> <sup>a</sup>
	Al	Si	P	
SAPO-34 precursor	30.7	44.7	24.6	3.23
Milled sample	39.4	28.9	31.7	—
Sample 2	39.8	21.9	38.3	1.78
Sample 6	42.5	13.5	44.0	1.63
SAPO-34-TEA <sup>b</sup>	45.3	20.6	34.1	2.76

<sup>a</sup> *R* = Si/(Al + P)<sub>surface</sub>/Si/(Al + P)<sub>bulk</sub>. <sup>b</sup> SAPO-34 synthesized with TEA as a template for comparison. Its bulk composition (Al<sub>0.486</sub>Si<sub>0.080</sub>P<sub>0.434</sub>O<sub>2</sub>) is similar to that of sample 6.

also confirmed by comparing with the surface composition of SAPO-34-TEA, which was synthesized by a conventional method and had similar bulk composition to sample 6 (Table 2). Based on the above results, it is thus concluded that the prolonged catalyst lifetime, improved selectivity to light olefins together with suppressed propylene hydrogenation to propane should be related to a combination of enhanced utilization of the internal pore space and reduced acidity caused by the reduced Si content especially the Si content on the external surface of the nanosized catalysts.

Besides the success in preparation of SAPO-34 nanocrystals, nanoscale SAPO-5 and SAPO-35 have been synthesized through this top-down route; for more details see ESI† (Fig. S7 and S8). These results demonstrate that the above method is universally applicable to SAPO molecular sieves.

In summary, SAPO molecular sieves with small crystal size have been prepared by an effective post-synthesis milling and recrystallization method. The mother liquid from zeolite production could be directly used as a recrystallization solution. The Si content in the product can be tuned by changing the recrystallization conditions. The considerably improved catalytic performance of SAPO-34 nanocrystals in the MTO reaction resulted from the shortened diffusion paths, decreased acid concentration, and reduced Si enrichment on the crystal surface. More useful nanosized molecular sieves are expected to be prepared using this facile and promising top-down strategy.

We thank the financial support from National Natural Science Foundation of China (21101150 and 20901076).

## Notes and references

- 1 A. Corma, *Chem. Rev.*, 1997, **97**, 2373.
- 2 (a) Z. Wang, J. Yu and R. Xu, *Chem. Soc. Rev.*, 2012, **41**, 1729; (b) J. Yu and R. Xu, *Acc. Chem. Res.*, 2010, **43**, 1195.
- 3 A. Corma, *J. Catal.*, 2003, **216**, 298.
- 4 (a) L. Tosheva and V. P. Valtchev, *Chem. Mater.*, 2005, **17**, 2494; (b) K. Na, M. Choi and R. Ryoo, *Microporous Mesoporous Mater.*, 2013, **166**, 3; (c) V. Valtchev and L. Tosheva, *Chem. Rev.*, 2013, **113**, 6734.
- 5 (a) B. M. Lok, C. A. Messina, R. L. Patton, R. T. Gajek, T. R. Cannan and E. M. Flanigen, *J. Am. Chem. Soc.*, 1984, **106**, 6092; (b) J. Liang, H. Y. Li, S. Zhao, W. G. Guo, R. H. Wang and M. L. Ying, *Appl. Catal.*, 1990, **64**, 31; (c) A. J. Marchi and G. F. Froment, *Appl. Catal.*, 1991, **71**, 139.
- 6 G. Yang, Y. Wei, S. Xu, J. Chen, J. Li, Z. Li, J. Yu and R. Xu, *J. Phys. Chem. C*, 2013, **117**, 8214.
- 7 H. van Heyden, S. Mintova and T. Bein, *Chem. Mater.*, 2008, **20**, 2956.
- 8 Y. Hirota, K. Murata, S. Tanaka, N. Nishiyama, Y. Egashira and K. Ueyama, *Mater. Chem. Phys.*, 2010, **123**, 507.
- 9 S. Lin, J. Li, R. P. Sharma, J. Yu and R. Xu, *Top. Catal.*, 2010, **53**, 1304.
- 10 S. Askari and R. Halladj, *Ultrason. Sonochem.*, 2012, **19**, 554.
- 11 P. Wang, D. Yang, J. Hu, J. a. Xu and G. Lu, *Catal. Today*, 2013, **212**, 62.e1.
- 12 V. Valtchev, G. Majano, S. Mintova and J. Perez-Ramirez, *Chem. Soc. Rev.*, 2013, **42**, 263.
- 13 (a) T. Wakihara, A. Ihara, S. Inagaki, J. Tatami, K. Sato, K. Komeya, T. Meguro, Y. Kubota and A. Nakahira, *Cryst. Growth Des.*, 2011, **11**, 5153; (b) T. Wakihara, R. Ichikawa, J. Tatami, A. Endo, K. Yoshida, Y. Sasaki, K. Komeya and T. Meguro, *Cryst. Growth Des.*, 2011, **11**, 955.
- 14 G. Liu, P. Tian, Y. Zhang, J. Li, L. Xu, S. Meng and Z. Liu, *Microporous Mesoporous Mater.*, 2008, **114**, 416.
- 15 (a) Z. Yan, B. Chen and Y. Huang, *Solid State Nucl. Magn. Reson.*, 2009, **35**, 49; (b) L. Zhang, J. Bates, D. Chen, H.-Y. Nie and Y. Huang, *J. Phys. Chem. C*, 2011, **115**, 22309.
- 16 D. Mores, E. Stavitski, M. H. F. Kox, J. Kornatowski, U. Olsbye and B. M. Weckhuysen, *Chem.-Eur. J.*, 2008, **14**, 11320.
- 17 P. Tian, B. Li, S. Xu, X. Su, D. Wang, L. Zhang, D. Fan, Y. Qi and Z. Liu, *J. Phys. Chem. C*, 2013, **117**, 4048.